Supporting Information

Self-supported Ru doped $NiMoO_4$ for efficient hydrogen evolution with 1000 mA cm^{-2} at a low overpotential

Pengfei Xue [a], *Man Qiao** [a], *Juhong Miao* [a], *Yujia Tang* [a], *Dongdong Zhu** [a] *and Chunxian Guo**[b]

[a] School of Chemistry and Materials Science, Institute of Advanced Materials and Flexible Electronics (IAMFE), Nanjing University of Information Science and Technology, Nanjing 210044, China
E-mail: dd.zhu@nuist.edu.cn, qiaoman@nuist.edu.cn

[b] Institute of Materials Science and Devices, School of Materials Science and Engineering, Suzhou University of Science and Technology, Suzhou 215009, China
E-mail: cxguo@usts.edu.cn

1 Experimental Section

1.1 Materials

Sodium hydroxide (NaOH), and Ruthenium (III) chloride hydrate ($RuCl_3 \cdot H_2O$) were purchased from Aladdin Ltd. (Shanghai, China). Ammonium persulfate ($(NH_4)_2S_2O_8$), hydrochloric acid (HCl), and absolute ethanol (C_2H_5OH) were bought from China National Pharmaceutical Group Corp. (China). All reagents used in this work were analytical grade without further purification. Milli-Q water with a resistance of 18.2 MΩ was used in all experiments.

1.2 Preparation of Ru-$NiMoO_4$

A piece of NiMo foam (2 cm × 3 cm) was ultrasonicated in 2.0 M hydrochloric acid, absolute ethanol, and Milli-Q for 10 min, respectively. Firstly, 3.0 g of sodium hydroxide, and 6.0 g of ammonium persulfate were added into 50 ml of Milli-Q water to form a transparent solution by magnetic stirring. Then the pretreated NiMo foam was immersed into the above oxidation solution for 20 h at ambient temperature. The obtained NiMo-based precursor (NiMo-Pre) was washed repeatedly using Milli-Q water and absolute ethanol, and dried in air naturally. Secondly, the obtained NiMo-Pre was immersed in 20 mM $RuCl_3$ solution under ambient conditions for 20 h to undergo a cation exchange process. Afterwards, the immersed sample was taken out, and washed repeatedly with Milli-Q water and absolute ethanol, and dried at 60 ℃. Finally, the obtained sample was annealed in an Ar atmosphere at 250 °C for 1.0 h to obtain Ru-$NiMoO_4$.

1.3 Preparation of $NiMoO_4$

The preparation of $NiMoO_4$ is similar to that of Ru-$NiMoO_4$, except the cation exchange process. In detail, 3.0 g of sodium hydroxide, and 6.0 g of ammonium persulfate were added into 50 ml of Milli-Q water to form a transparent solution by magnetic stirring. Then the pretreated NiMo foam was immersed into the above oxidation solution for 20 h at ambient temperature. The obtained NiMo-based precursor (NiMo-Pre) was washed repeatedly using Milli-Q water and absolute ethanol, and dried in air naturally. Afterwards, $NiMoO_4$ was fabricated by annealing NiMo-Pre in an Ar atmosphere at 250 °C for 1.0 h.

1.4 Characterizations

The morphology of the samples was characterized by field emission scanning electron microscopy (FESEM, Zeiss Gemini SEM 300) equipped with an energy dispersive spectrometer (EDS) and transmission electron microscopy (TEM, JEOL JEM-2100F). X-ray photoelectron spectroscopy (XPS) measurements were carried out on an ESCALab250 using Al Kα radiation, and the working voltage is 12.5 KV. The binding energy was calibrated to the C 1s peak of 284.8 eV.

1.5 Electrochemical measurements:

All the electrochemical measurements were carried out in a three-electrode system on a CHI 760E workstation (CH instrument, Shanghai, China) at ambient conditions. The Ru-$NiMoO_4$ supported on NiMo foam was directly used as the working electrode, while Hg/HgO electrode, and platinum foil were used as the reference, and counter electrodes, respectively. 1.0 M KOH aqueous solution was used as the electrolyte for the hydrogen evolution reaction test. Before data collection, the working electrode was scanned by cyclic voltammetry (CV) plots until the signal was stabilized. Linear sweep voltammetry (LSV) curves were recorded with a scan rate of 5.0 mV s^{-1}. The obtained current densities were normalized to the geometrical surface area. The reversible hydrogen electrode (RHE) potentials were obtained by the following equation: $E_{(RHE)} = E_{(Hg/HgO)} + 0.0592 \times pH + 0.098$. Electrochemical impedance spectroscopy (EIS) was measured in the frequency range from 0.1 Hz to 100 kHz with an amplitude of 5 mV at an initial potential of −1.1 V (vs. Hg/HgO). IR × 90% compensation of LSV curves was performed using the solution resistance estimated from EIS results. The double-layer capacitance (C_{dl}) of the samples were obtained from CV plots in a small non-faradaic region (from 0 to −0.1 V vs. Hg/HgO) at different scan rates (20, 40, 60, 80, 100, and 120 mV s^{-1}). The electrode durability was tested by the chronopotentiometry method (60 h), and chronoamperometry method (150 h), respectively. The HER polarization curves before and after 150 h chronoamperometry test were also collected.

2 Supplementary Figures and Tables

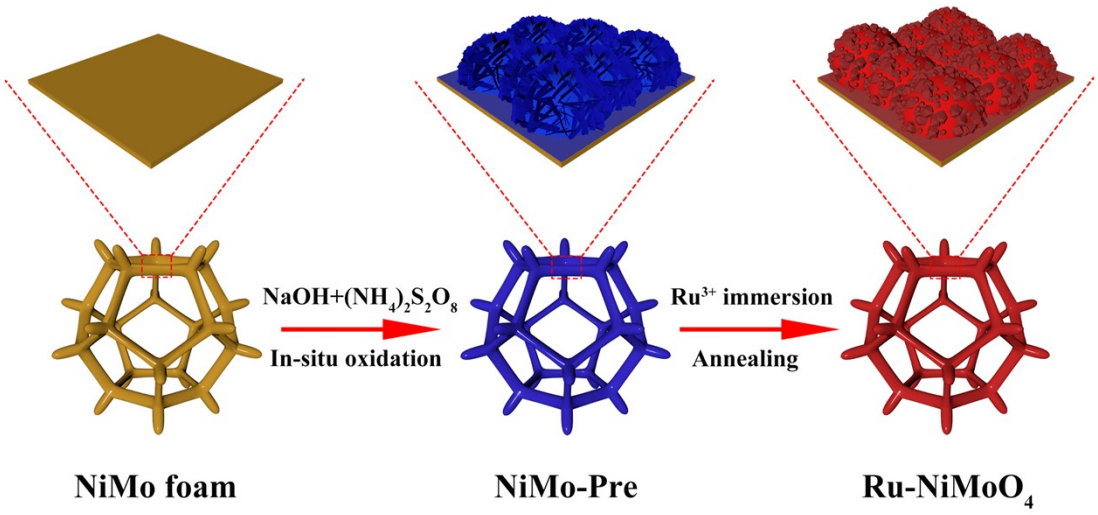

Figure S1. Schematic illustration of the synthesis process for Ru-$NiMoO_4$ on NiMo foam.

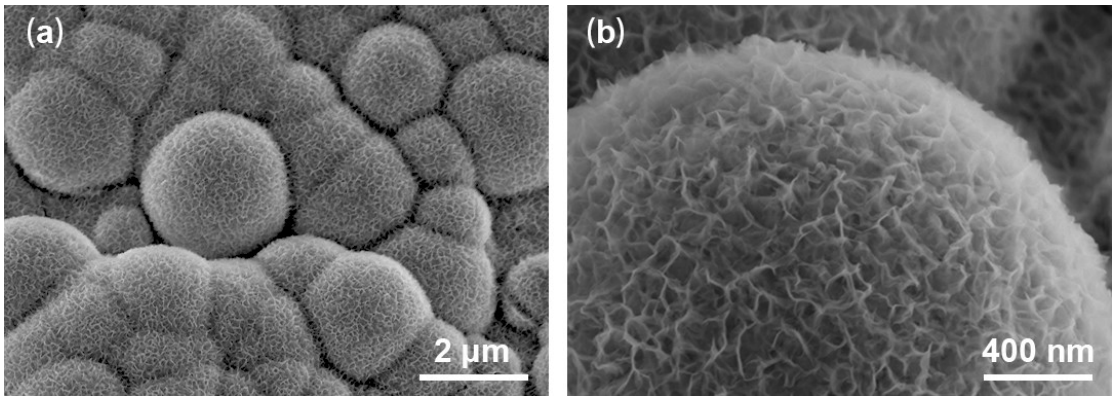

Figure S2. SEM images of NiMo-based precursor with different resolutions.

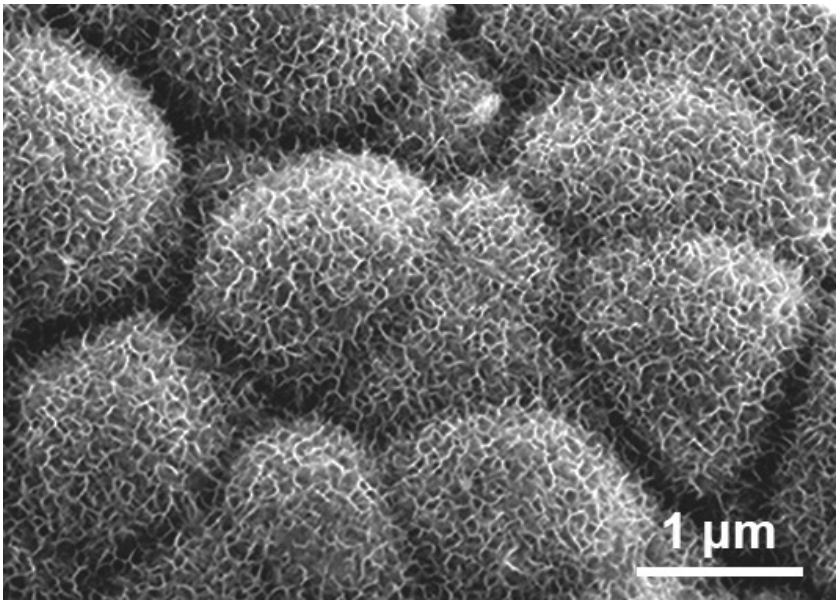

Figure S3. SEM image of $NiMoO_4$.

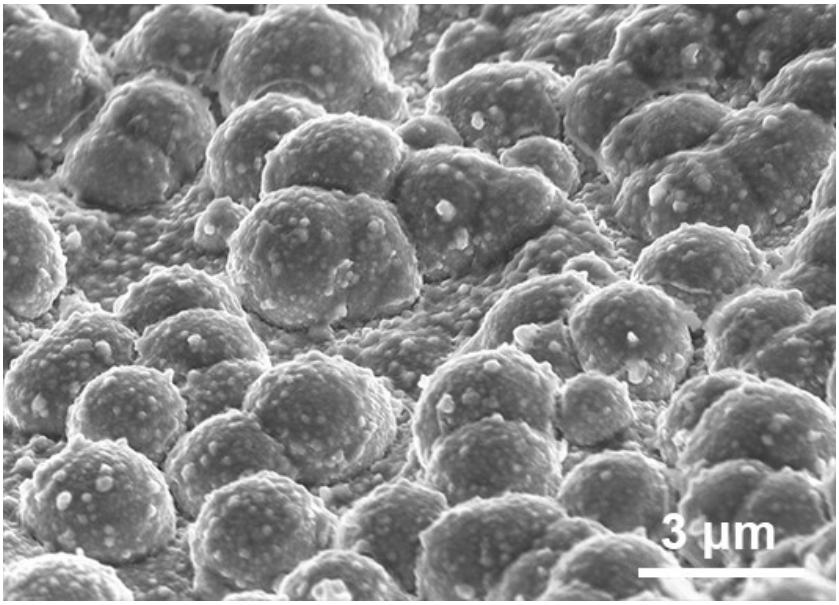

Figure S4. SEM image of Ru-$NiMoO_4$.

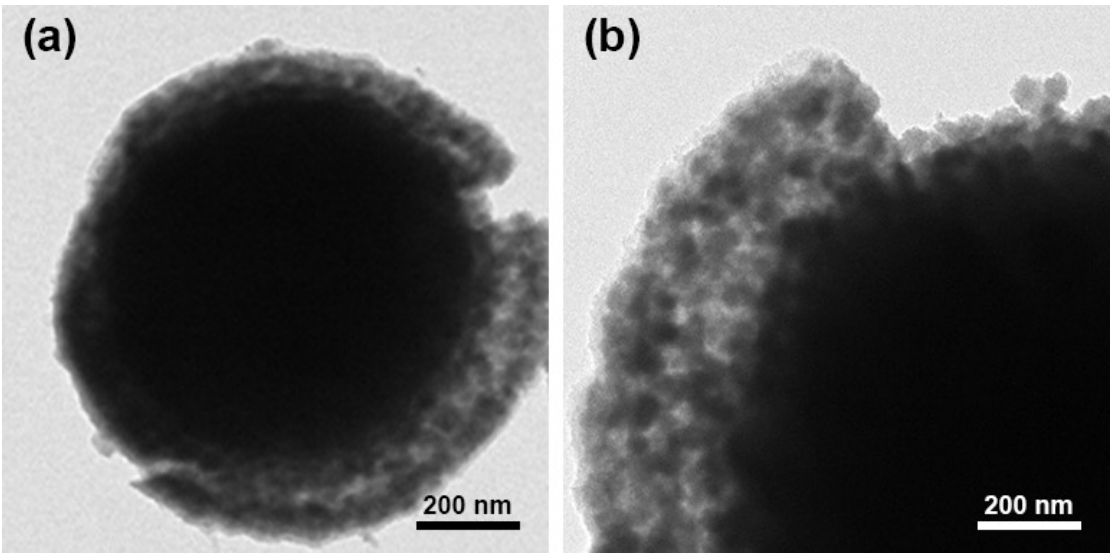

Figure S5. TEM images of Ru-$NiMoO_4$ with different resolutions.

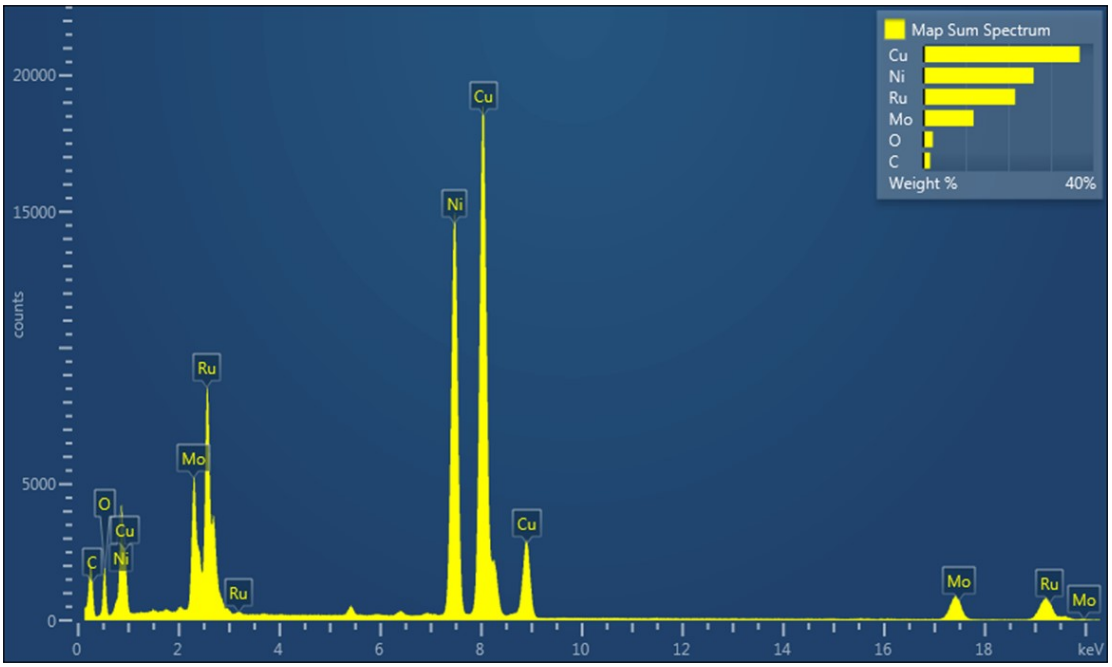

Figure S6. TEM-EDX spectrum of Ru-$NiMoO_4$. C and Cu signals are originated from the TEM support grid.

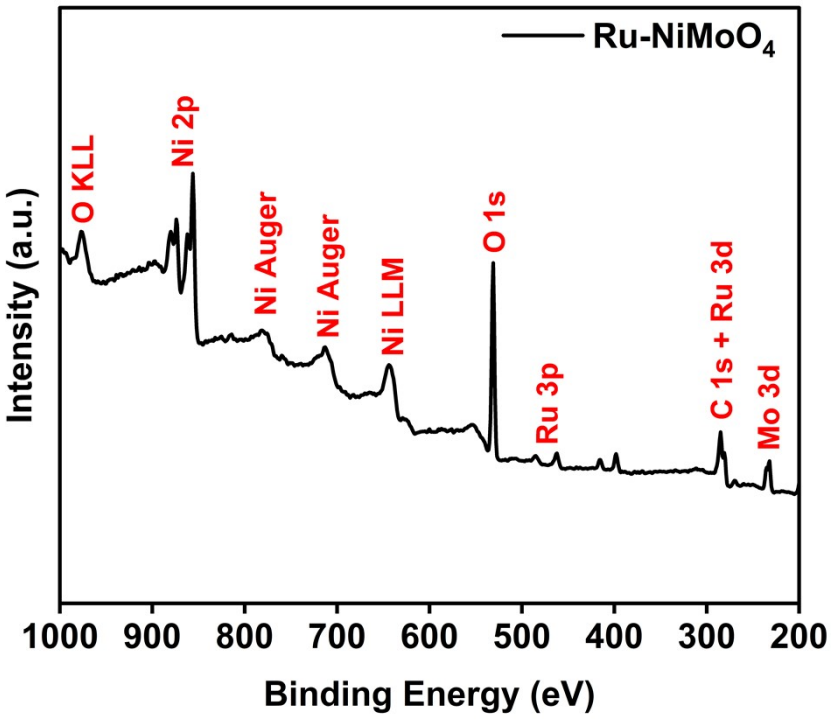

Figure S7. XPS survey spectrum of Ru-$NiMoO_4$.

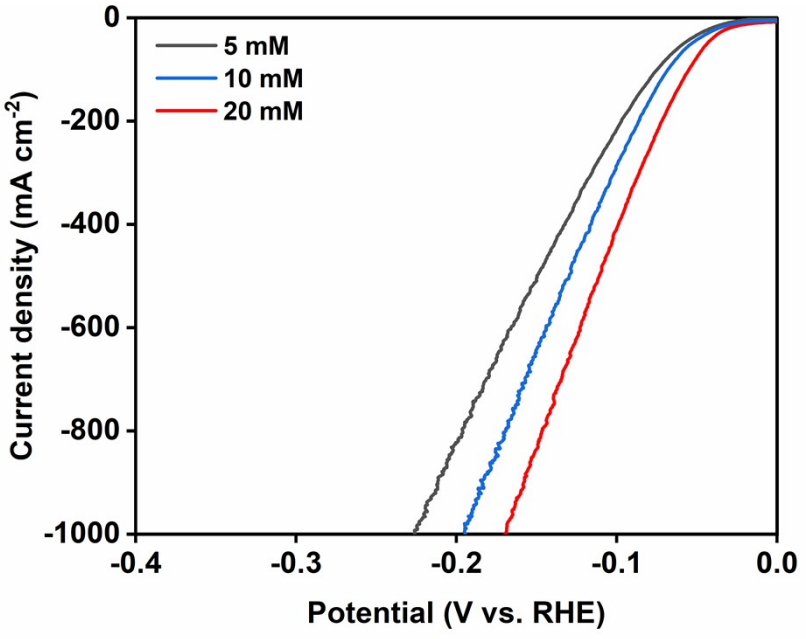

Figure S8. LSV curves of three Ru-$NiMoO_4$ samples synthesized by using 5, 10, or 20 mM $RuCl_3$ solution.

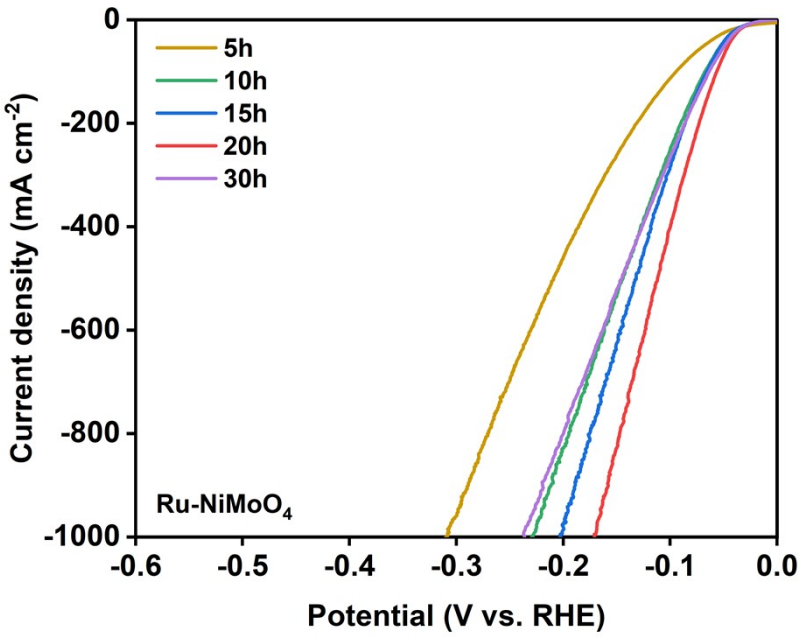

Figure S9. LSV curves of five Ru-$NiMoO_4$ samples synthesized by applying different immersion time (5, 10, 15, 20, or 30 h) in 20 mM $RuCl_3$ solution.

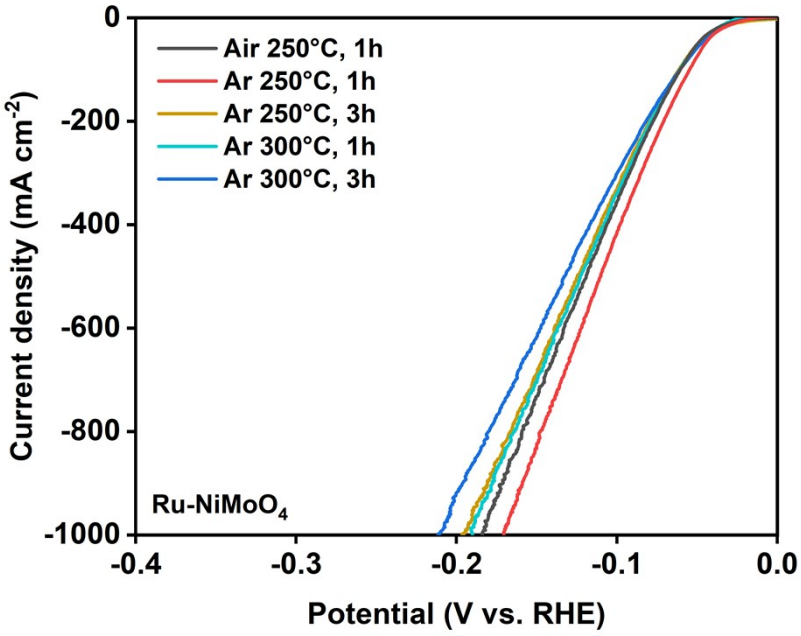

Figure S10. LSV curves of five Ru-$NiMoO_4$ samples synthesized by under different annealing conditions (Temperature: 250 or 300 ℃; Time: 1 or 3 h; Atmosphere: Argon or Air).

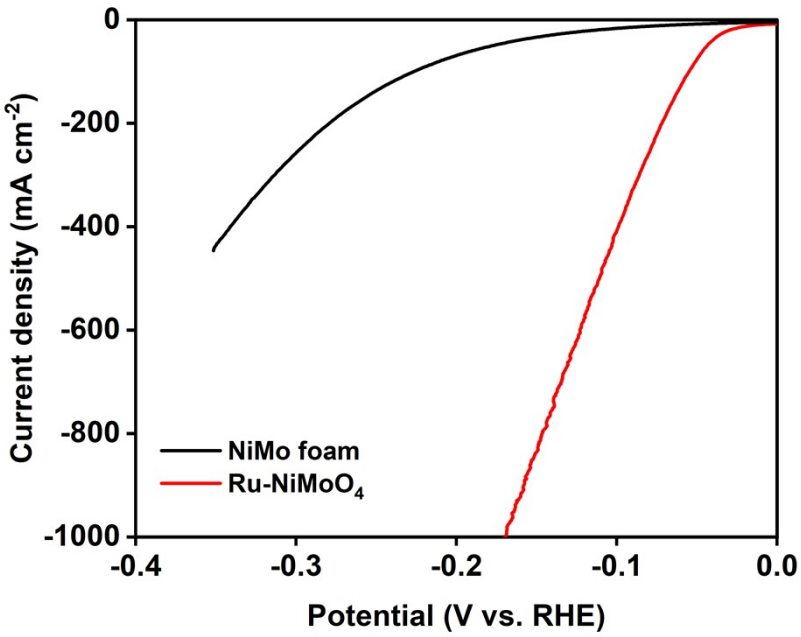

Figure S11. LSV curves of Ru-$NiMoO_4$, and commercial NiMo foam tested in 1.0 M KOH electrolyte.

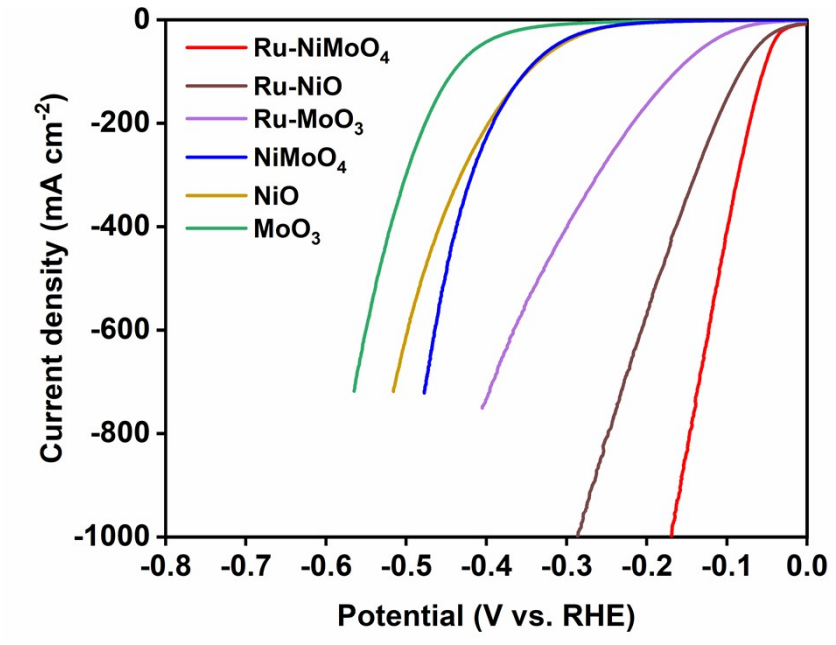

Figure S12. LSV curves of different samples tested in 1.0 M KOH electrolyte.

Ru-NiO, and Ru-MoO_3 samples were prepared via using the same material synthesis strategy for Ru-$NiMoO_4$, except that Ni foam and Mo foil were used as the starting substrate. NiO, MoO_3, and $NiMoO_4$ were also investigated for comparison. As shown in Fig. S12, compared to NiO and MoO_3, $NiMoO_4$ is more active for HER, suggesting that $NiMoO_4$ is a relatively good electrocatalyst for alkaline HER. Moreover, $NiMoO_4$ acts as a substrate to support dispersed Ru species, thus reducing the usage amount of noble metal Ru. Furthermore, Ru-$NiMoO_4$ sample has much higher HER activity than Ru-NiO, and Ru-MoO_3, highlighting the crucial role of $NiMoO_4$ support for alkaline HER.

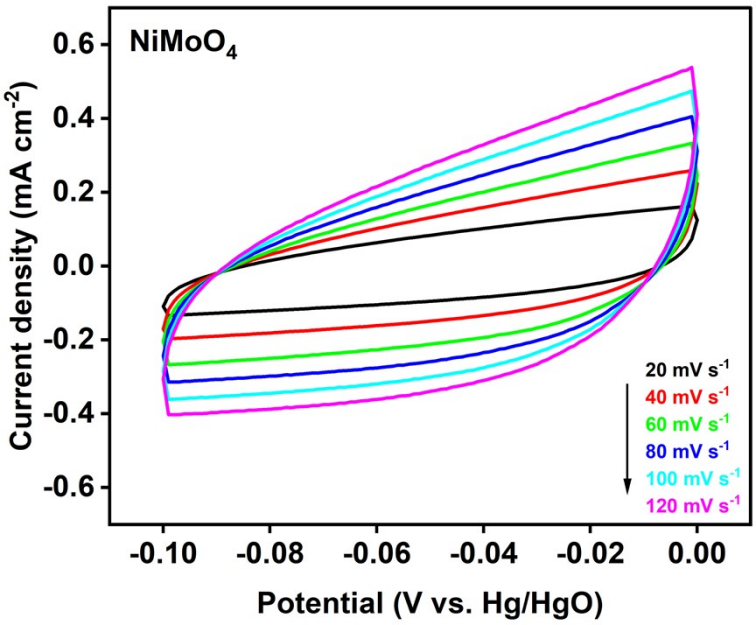

Figure S13. CV curves for $NiMoO_4$ at scan rates from 20 to 120 mV s^{-1}.

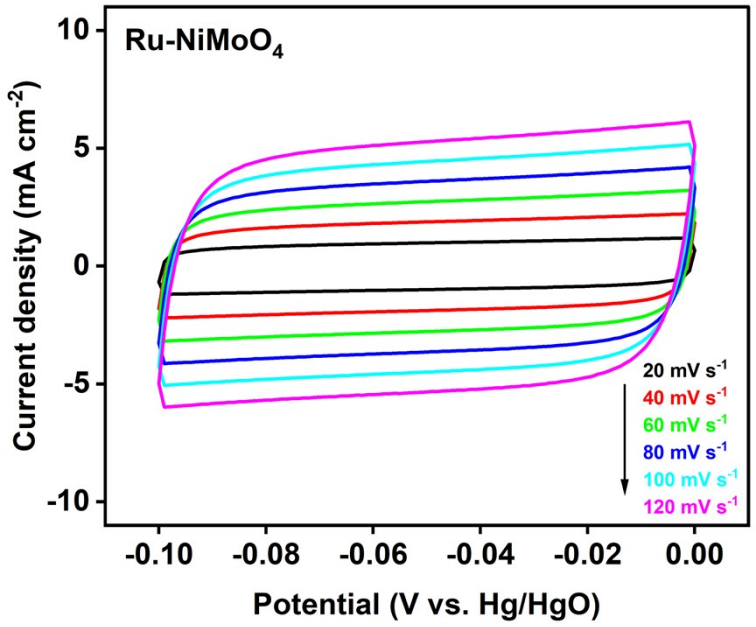

Figure S14. CV curves for Ru-$NiMoO_4$ at scan rates from 20 to 120 mV s^{-1}.

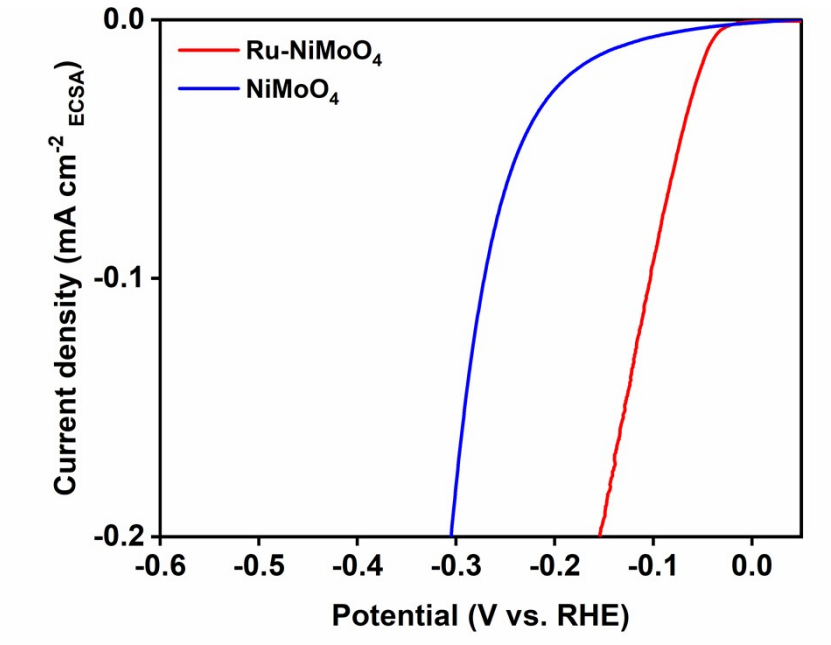

Figure S15. ECSA-normalized LSV curves of Ru-$NiMoO_4$, and $NiMoO_4$ in 1.0 M KOH electrolyte.

C_{dl} values are converted to electrochemical active surface area (ECSA) by the following equation: ECSA= C_{dl}/C_s. The specific capacitance(C_s) for a flat surface is generally in the range of 20-60 μF cm^{-2}, and here 40 μF cm^{-2} is used for calculation (*Angew. Chem. Int. Ed.*, 2014, 53, 14433–14437). Therefore, ECSAs of Ru-$NiMoO_4$, $NiMoO_4$ were calculated to be 1077.5, and 52.5 cm^2_{ECSA}, respectively. The ECSA-normalized LSV curves show that Ru-$NiMoO_4$ has enhanced intrinsic HER activity than $NiMoO_4$.

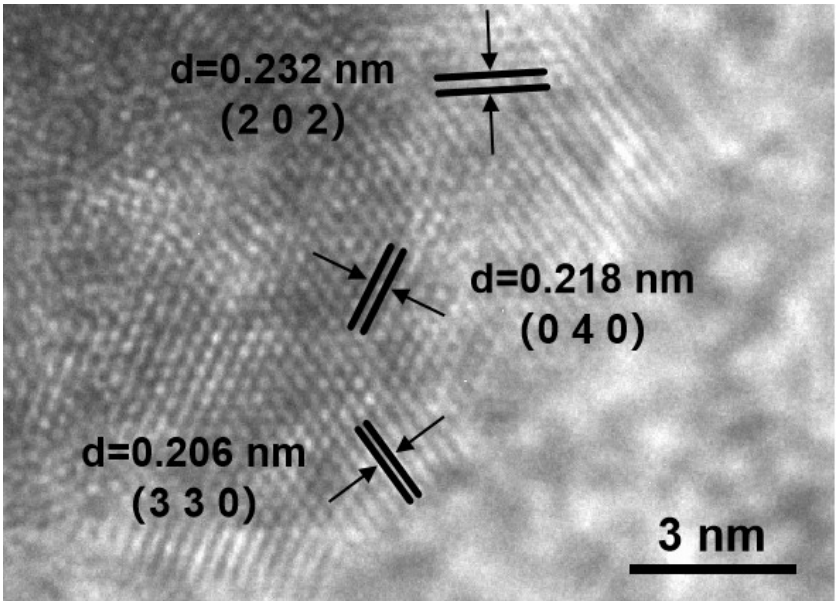

Figure S16. HRTEM image of Ru-$NiMoO_4$ sample after the HER cycling test.

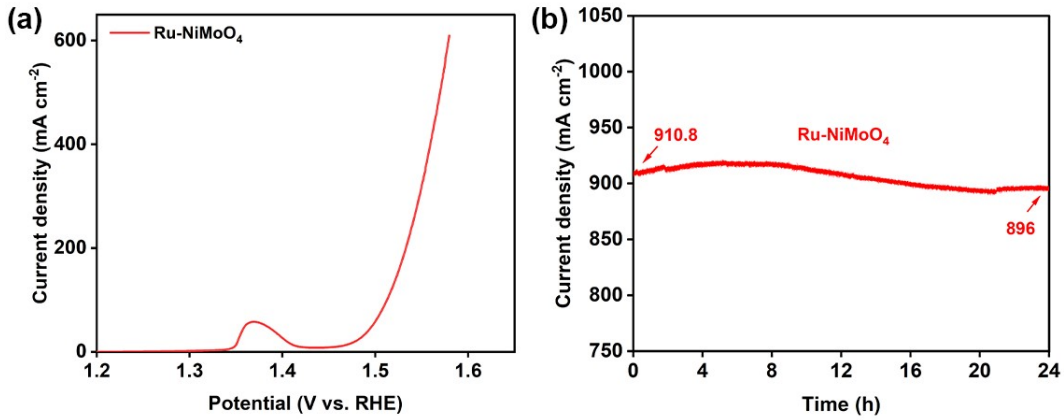

Figure S17. (a) OER polarization curve of Ru-$NiMoO_4$ in 1.0 M KOH electrolyte, (b) chronoamperometry curve of Ru-$NiMoO_4$ at a certain potential of 0.95 V vs. Hg/HgO for 24 hours.

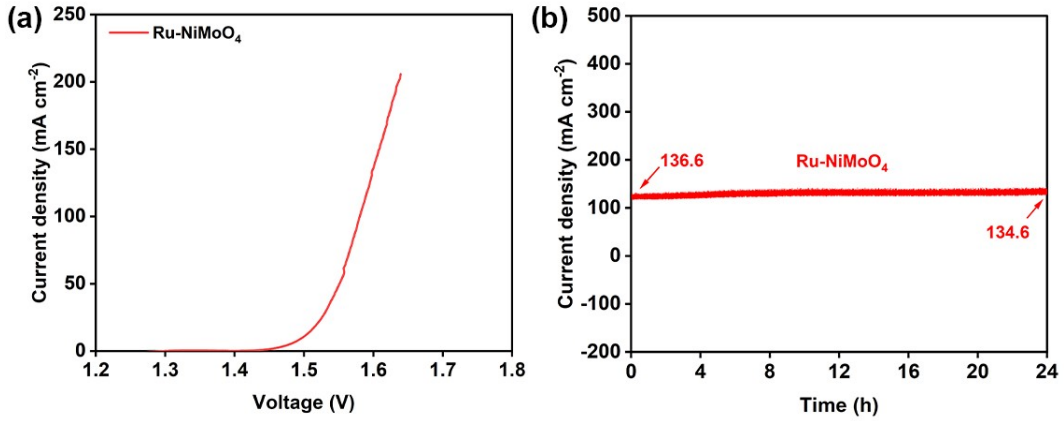

Figure S18. (a) Polarization curve of Ru-$NiMoO_4$ for overall water splitting in a two-electrode configuration, (b) chronoamperometry curve of Ru-$NiMoO_4$ for water electrolysis in 1.0 M KOH at 1.7 V.

Table S1. Comparison of HER activity of Ru-$NiMoO_4$ and some representative high current density HER electrocatalysts in alkaline solutions.

Catalyst	**Substrate**	**Overpotential (mV) at 1000 mA cm^{-2}**	**Tafel slope (mV dec^{-1})**	**Reference**
Ru-$NiMoO_4$	NiMo foam	170.6	26.4	This work
Ru-$NiSe_2$	Ni foam	180.8	28	[1]
Ru_3Ni	Carbon support	168	28	[2]
Sr_2RuO_4	Cu wire	278	22	[3]
Ru clusters	Carbon paper	196	25.3	[4]
Ru SACs/FeCo-LDH	Ni foam	117	53	[5]
Mo_2C/MoC	CNT film	233	42	[6]
Ru-CoO_x	Ni foam	252	28	[7]
β-NiMoHZ	Ni foam	210	44	[8]
Ru/(Fe, Ni)$(OH)_2$	Ni foam	152	30	[9]
Co/Se-MoS_2	carbon paper	382	67	[10]
NiO/RuO_2	Ni foam	178	42	[11]
IrNi-$FeNi_3$	Ni foam	288.8	67	[12]
Ru-Mo_2C	CNT film	78	26	[13]
Ni_3S_2/Cr_2S_3	Ni foam	227	87	[14]
FeIr	Ni foam	204	40.9	[15]
$NiMoO_x$/NiMoS	Ni foam	236	NA	[16]
MoS_2/Mo_2C	Ti foil	220	44	[17]
S-NiBDC	Ni foam	310	75	[18]

References

1. Y. Bai, H. Zhang, X. Lu, L. Wang, Y. Zou, J. Miao, M. Qiao, Y. Tang and D. Zhu, *Chem. Eur. J*, 2023, **29**, e202300205.
2. L. Gao, F. Bao, X. Tan, M. Li, Z. Shen, X. Chen, Z. Tang, W. Lai, Y. Lu, P. Huang, C. Ma, S. C. Smith, Z. Ye, Z. Hu and H. Huang, *Energy Environ. Sci*, 2023, **16**, 285−294.
3. Y. Zhang, K. E. Arpino, Q. Yang, N. Kikugawa, D. A. Sokolov, C. W. Hicks, J. Liu, C. Felser and G. Li, *Nat. Commun*, 2022, **13**, 7784.
4. Q. Hu, K. Gao, X. Wang, H. Zheng, J. Cao, L. Mi, Q. Huo, H. Yang, J. Liu and C. He, *Nat. Commun*, 2022, **13**, 3958.
5. X. Mu, X. Gu, S. Dai, J. Chen, Y. Cui, Q. Chen, M. Yu, C. Chen, S. Liu and S. Mu, *Energy Environ. Sci*, 2022, **15**, 4048−4057.
6. C. Li, Z. Wang, M. Liu, E. Wang, B. Wang, L. Xu, K. Jiang, S. Fan, Y. Sun, J. Li and K. Liu, *Nat. Commun*, 2022, **13**, 3338.
7. D. Wu, D. Chen, J. Zhu and S. Mu, *Small*, 2021, **17**, 2102777.
8. Z. Wang, J. Chen, E. Song, N. Wang, J. Dong, X. Zhang, P. M. Ajayan, W. Yao, C. Wang, J. Liu, J. Shen and M. Ye, *Nat. Commun*, 2021, **12**, 5960.
9. X. Xiao, X. Wang, X. Jiang, S. Song, D. Huang, L. Yu, Y. Zhang, S. Chen, M. Wang, Y. Shen and Z. Ren, *Small Methods*, 2020, **4**, 1900796.
10. Z. Zheng, L. Yu, M. Gao, X. Chen, W. Zhou, C. Ma, L. Wu, J. Zhu, X. Meng, J. Hu, Y. Tu, S. Wu, J. Mao, Z. Tian and D. Deng, *Nat. Commun*, 2020, **11**, 3315.
11. T. Yu, Q. Xu, L. Luo, C. Liu and S. Yin, *Chem. Eng. J*, 2022, **430**, 133117.
12. Y. Wang, G. Qian, Q. Xu, H. Zhang, F. Shen, L. Luo and S. Yin, *Appl. Catal. B,* 2021, **286**, 119881.
13. X. Wu, Z. Wang, D. Zhang, Y. Qin, M. Wang, Y. Han, T. Zhan, B. Yang, S. Li, J. Lai and L. Wang, *Nat. Commun*, 2021, **12**, 4018.
14. H. Q. Fu, M. Zhou, P. F. Liu, P. Liu, H. Yin, K. Z. Sun, H. G. Yang, M. Al-Mamun, P. Hu, H.-F. Wang and H. Zhao, *J. Am. Chem. Soc*, 2022, **144**, 6028−6039.
15. F. Shen, Y. Wang, G. Qian, W. Chen, W. Jiang, L. Luo and S. Yin, *Appl. Catal. B*, 2020, **278**, 119327.
16. P. Zhai, Y. Zhang, Y. Wu, J. Gao, B. Zhang, S. Cao, Y. Zhang, Z. Li, L. Sun and J. Hou, *Nat. Commun*, 2020, **11**, 5462.
17. Y. Luo, L. Tang, U. Khan, Q. Yu, H.-M. Cheng, X. Zou and B. Liu, *Nat. Commun*, 2019, **10**, 269.
18. F. Cheng, X. Peng, L. Hu, B. Yang, Z. Li, C.-L. Dong, J.-L. Chen, L.-C. Hsu, L. Lei, Q. Zheng, M. Qiu, L. Dai and Y. Hou, *Nat. Commun*, 2022, **13**, 6486.